Aerosol - Cloud Target Classification in HALO Lidar/Radar Collocated Measurements

Eleni Marinou, Florian Ewald, Silke Gross, Martin Wirth, Andreas Schaefler, Quitterie Cazenave, Julien Delanoë

AEROSOL - CLOUD TARGET CLASSIFICATION IN HALO LIDAR/RADAR COLLOCATED MEASUREMENTS

Eleni Marinou[1*], Florian Ewald[1], Silke Gross[1], Martin Wirth[1], Andreas Schaefler[1], Quitterie Cazenave[2] and Julien Delanoë[2]

[1] *Deutsches Zentrum für Luft- und Raumfahrt (DLR), Institut für Physik der Atmosphäre, Oberpfaffenhofen 82234, Germany.*

[2]*Laboratoire Atmosphères, Milieux, Observations Spatiales, Guyancourt, France*

*Email: Eleni.Marinou@dlr.de

ABSTRACT

Particle attenuated backscatter and depolarization ratio at 532 nm from the WALES (Water Vapor Lidar Experiment in Space) instrument are used in combination with the radar reflectivity from the 35 GHz MIRA35 cloud radar in order to perform an aerosol-cloud target classification on the lidar/radar collocated observations carried out with the High Altitude and LOng-range research aircraft (HALO), in high temporal and spatial resolution.

The methodology is applied to the measurements conducted during the North Atlantic Waveguide and Downstream Impact Experiment (NAWDEX) in fall 2016. Here, we present one case study to show the feasibility and information context of the aerosol-cloud discrimination, which can serve as a good complement to the Cloud target categorization applied already in the measurements. Our results demonstrate that the developed mask is capable to identify complex stratifications with different aerosol and cloud types and even aerosol layers of low signal.

1. INTRODUCTION

Aerosol, clouds and their interactions with each other, but also with radiation and precipitation, influence weather and climate. Aerosols act as cloud condensation nuclei and ice nuclei influencing the cloud macro- and micro-physical properties and precipitation initiation. Despite of the significant influence aerosols and clouds have on climate, the quantification of their effect presents a large uncertainty, which can be partly attributed to their spatiotemporal variability and the diversity of the occurring processes [1].

In order to better quantify the aerosols and clouds effect on climate, and to improve the determination of their interactions, high spatiotemporal and vertically resolved observations of these features are of great assistance. Lidar/radar collocated measurements of aerosols and clouds is of unprecedented significance towards this goal. Several synergistic observations are currently utilized under this concept, applied at the framework of ground-based Research Infrastructures (e.g. ACTRIS, ARM) and at airborne and space platforms (e.g. HALO, RALI, CALIPSO, CLOUDSAT).

For an in-depth study of the aerosol and cloud properties observed with the aforementioned synergistic datasets, the atmospheric features detected are primarily classified as aerosols or clouds, based on lidar-only or synergistic lidar/radar categorization methods [e.g. 2, 3, 4]. For the HALO observations, a sophisticated aerosol classification has been developed [5] and a cloud classification scheme [6] has been implemented. However, there is no aerosol-cloud target classification scheme which will be used in combination to the other two categorizations to further assess aerosol and clouds features and study their interactions. Motivated by this need, we aim to develop a basic aerosol-cloud categorization of the observed features, utilizing the collocated airborne lidar and radar measurements. To this end, we use key parameters estimated by the two systems, which are independent of calibration sensitivities that may vary from flight-to-flight operations. The basic quantities used are the particle attenuated backscatter coefficient (β_{par}) and particle depolarization ratio (δ_{par}) at 532 nm from the lidar, and the radar reflectivity (Z_e) from the cloud radar.

To develop the classification mask and demonstrate its' performance, we use the datasets obtained during the NAWDEX experiment,

including collocated lidar-radar aerosol and cloud observations from overflights of the North Atlantic Ocean for a period of one month. From this dataset we derive the β_{par}, δ_{par} and Z_e parameters and perform the aerosol-cloud classification of the atmospheric features, in high temporal resolution. In the future, this basic typing will be used for detecting the necessary features, as for example on the aerosol-cloud-interaction processes and on the retrieval of aerosols and clouds optical and microphysical properties [e.g. 4, 7].

The work is structured as follows: first, the NAWDEX experiment is briefly introduced in section 2.1, then the methodology to derive the aerosol-cloud categorization is described in section 2.2. The methodology is applied and analyzed in section 3, and conclusions and future work are drawn in Section 4.

2. METHODOLOGY

2.1 NAWDEX

The North Atlantic Waveguide and Downstream Impact Experiment (NAWDEX) was conducted above the domain [70W – 10E; 45N – 80N] during 17/9 to 22/10 of 2016 [8]. In this campaign, four aircrafts were deployed with a sophisticated remote-sensing and in-situ payload and ground-based measurements. For this study, the dataset collected with the HALO are used, and particularly the lidar observations from the WALES instrument [9] and the cloud radar observations of the MIRA-35 instrument of HAMP (HALO Microwave Package) [10]. During the campaign, HALO performed 16 flights with a total of 96 flight hours and the observations include low, medium and high level clouds (ice, water and mixed phase) along with several marine and elevated aerosol layers in between the clouds.

2.2 Aerosol Classification

In order to demonstrate the quantities used for the aerosol - cloud classification, the time-height cross sections of these quantities are shown in Figure 1 for the day of 27/9/2016. The atmospheric features are well seen in the radar reflectivity (1-tob) the particulate attenuated backscatter coefficient (1-center) and the particle depolarization ratio (1-bottom). Several ice clouds are visible (up to 8 km) along with water clouds

(bellow ~4 km). Between the clouds, two distinctive aerosol layers are observed, one between 15:00 and 16:00 UTC with $\beta_{par} > 10^{-6} m^{-1} sr^{-1}$ and enhanced δ_{par} (30 ± 3%) and one between 16:30 to 17:30 UTC with low attenuation ($< 10^{-6} m^{-1} sr^{-1}$) and depolarization (between ~3% and 18%).
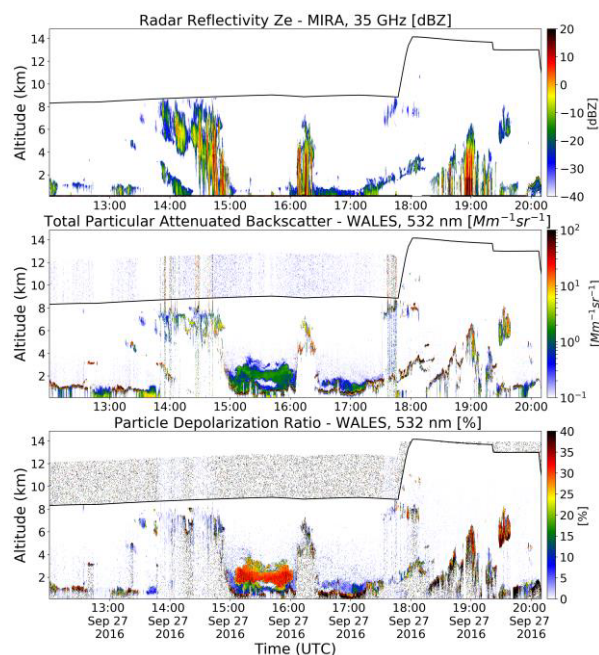

Figure 1. HALO observations at NAWDEX on 27/9/2016. From top to bottom: MIRA35 cloud radar reflectivity, WALES particle attenuated backscatter coefficient at 532 nm and WALES particle depolarization ratio at 532 nm.

For the typing of atmospheric features, i.e. the optical dominant scattered type, Z_e, β_{par} and δ_{par} observations are used for the classification between aerosols and clouds. Auxiliary to the observations, the temperature, pressure and water vapor fields from the ECMWF ensemble (European Center from Medium Range Weather Forecast) is used. The complete typing procedure is listed in Table 1 and is described below. Overall, the classification is based on 60 m vertical and 5 sec (~ 1 km) averaged profiles of lidar and radar observations.

In the first step, the classification utilizes the cloud radar observations and where a feature is detected from the radar (Z_e not equal to the fill value), this feature is consider to be cloud, surface or insects and its specific classification is handled by the methodology described in [6]. For the bits where both lidar and radar signals are totally

attenuated, the cell is categorized as present of liquid unknown (same as in [6]). The atmosphere is classified as clear sky if $\beta_{par} < 1 \times 10^{-8}m^{-1}sr^{-1}$, a threshold which is well below the given range of aerosols of the CALIPSO classification [11]. The observations with $\beta_{par} > 2 \times 10^{-5}m^{-1}sr^{-1}$ are classified as clouds, a well suited threshold for the discrimination between aerosols and clouds, as the largest overlap between the two features is found in the β_{par} region between $4 \times 10^{-6}m^{-1}sr^{-1}$ and $1 \times 10^{-5}m^{-1}sr^{-1}$ [12]. This threshold value in the β_{par} is also used in the Cloudnet for the discrimination between aerosols and clouds [3]. Utilizing the δ_{par} , the lidar observations with $\delta_{par} < 1\%$ are considered to be water clouds and with $\delta_{par} > 38\%$ ice clouds.

The aforementioned decisions are based on each lidar/radar observational bin. Furthermore, some filters are applied to account for the Cirrus fringes and the features coherence. The filters are described hereon.

Cirrus fringes for tenuous ice clouds: If in a target bin the temperature is less than 0°C and the bin is adjusted to an ice cloud (within the ± 180 m vertical and ± 2 km horizontal window), then the target bin is categorized as cirrus (similar as "Fringe amelioration" in CALIPSO [4] and in Cloudnet [3] categorizations).

Coherent filter for clear sky: if in the 3x3 cell around a target bin there are more than 5 bins (out of the total 9) that are categorized as clear sky (from the previous filters), the bin of interest is considered to be clear sky. This filter deals with the random molecular nose.

Coherent filter for clouds: if in a 3x3 cell around a target bin there are more that 5 bins (out of the total 9) that are categorized as clouds, the bin of interest is considered to be cloud.

Coherent filter for aerosols: if in a 3x3 cell around a target bin there are less than 4 bins (out of the total 9) that are categorized as clouds, clear sky, totally attenuated, surface or insects, the bin of interest is considered to be aerosols.

The remaining observations that are not categorized as clouds, clear sky, totally attenuated, surface or insects are considered to be aerosols.

Table 1. Overview of feature typing.

Aerosol – Cloud target classification
If detected Z_e: Clouds, surface and/or insects
If lidar and radar signals are totally attenuated: presence of liquid unknown
If $\beta_{par} > 2 \times 10^{-5}m^{-1}sr^{-1}$: Clouds
If $\beta_{par} < 1 \times 10^{-8}m^{-1}sr^{-1}$: Clear sky
If $\delta_{par} < 1\% \ or \ > 38\%$: Clouds
If T < 0 and there is an adjusted cloud: Cirrus fringe
If in the 3x3 cell around a target bin clear sky prevail: Clear sky
If in the 3x3 cell around a target bin clouds prevail: Clouds
If in the 3x3 cell around a target bin aerosols prevail: Aerosols
All the remaining uncategorized targets: Aerosols

[*] Further cloud sub-classification is applied with [6]

3. RESULTS

3.1 Aerosol cloud separation

In this section, we demonstrate the aerosol – cloud separation acquired with the discussed classification, for the flight of 27/9/2016. Figure 3 shows the distributions of occurrence frequency of the WALES measurements on the 2D space of $log_{10}(\beta_{par})$ vs δ_{par} for all features (top), for the features categorized as aerosols (bottom-left) and for the features categorized as clouds (bottom-right). The aerosol layers in this case occupied mainly the β_{par} area between $10^{-6.5} - 10^{-5.5}$ with δ_{par} as high as 36%, indicating a dust layer. Although the aerosol measurements with $\beta_{par} < 10^{-6.5}$ are acquired with low confidence, they are still included in the aerosol class. In the clouds 2D β_{par} vs δ_{par} space, we can distinguish the water clouds region with $\delta_{par} < 5\%$ and the cirrus region with $\delta_{par} > 20\%$.

3.2 The new target classification

In Figure 3 we demonstrate the aerosol – cloud separation acquired with the discussed target categorization, along with its' combination with the cloud sub-categorization of [6], for the discussed case of 27/9/2016. We see that the aerosol and cloud features are successfully detected and separated. With the combination of the cloud sub-categorization mask, we observe the

several liquid clouds (purple color) above the domain up to 4km, and the aerosol layers (orange color) which are located right on top of the water clouds between 13:45 to 17:15 UTC. Exactly before and after the dust observations, ice clouds are detected (blue color), elevated up to 7 km.
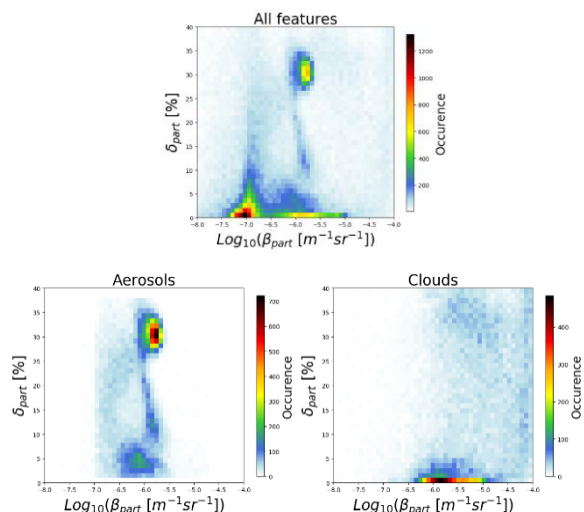

Figure 2. Distribution of occurrence frequency as a function of $log_{10}(\beta_{par})$ and δ_{par} for all the observations (top), the aerosols (bottom-left) and the clouds (bottom-right), for the WALES observations on 27/9/2018.
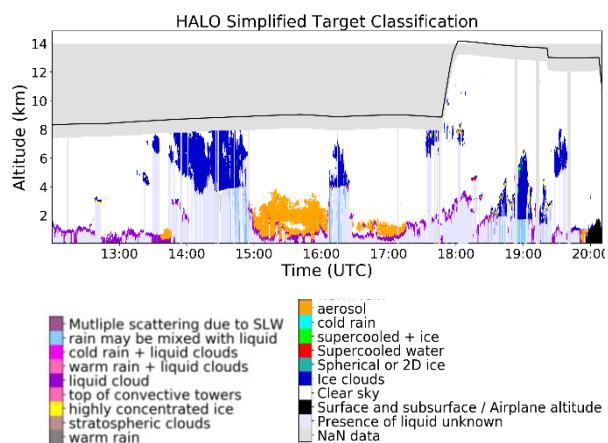

Figure 3. Target classification for 27/9/2016.

4. CONCLUSIONS

In this work, we combine lidar and radar observations from the HALO platform with high temporal and spatial resolution, with the scope to categorize the detected atmospheric features in aerosols and clouds. For the demonstration of the classification, we apply our methodology on data collected during the NAWDEX experiment. We conclude that the variables of the radar reflectivity, the particulate attenuated backscatter coefficient

and the particle depolarization ratio at 532 nm are sufficient to discriminate aerosol and cloud features. The new target categorization works well and is in agreement with Cloudnet aerosol-cloud categorization. More cases will be analyzed, in a variety of atmospheric conditions and aerosol loads so as to further evaluate the performance of the new mask. Additionally, the mask will be combined with the HALO aerosol mask presented in [5] for a complete aerosol and cloud characterization of the scenes.

ACKNOWLEDGEMENTS

REFERENCES

[1] Seinfeld, et al., PNAS,113 (21) 5781-5790 (2016)
[2] Baars et al., Atmos. Meas. Tech., 10, 3175-3201 (2017)
[3] Hogan and O'Connor, Dept. of Meteorol. Univ. of Reading, UK, available at: http://www.met.reading.ac.uk/~swrhgnrj/publications/ categorization.pdf (last access: March 2019) (2004)
[4] Liu et al., Atmos. Meas. Tech., 12, 703-734 (2019)
[5] Gross et al., Atmos. Chem. Phys., 13, 2487–2505 (2013)
[6] Ceccaldi et al., J. Geophys. Res. Atmos.,118, 7962–7981 (2013)
[7] Cazenave et al., Atmos. Meas. Tech. Discuss., in review (2018)
[8] Schäfler, et al., Bull. Amer. Meteor. Soc., 99, 1607–1637 (2018)
[9] Wirth et al., Appl. Phys. B, 96, 201-213 (2009)
[10] Ewald, et al., Atmos. Meas. Tech. Discuss., in review (2018)
[11] Winker et al., Atm. Ocean. Tech., 26, 2310-2323 (2009)
[12] Liu et al., J. Atmos. Oceanic Technol., 26, 1198–1213 (2009)